Stratifin as a Novel Diagnostic Biomarker in Serum for Diffuse Alveolar Damage

Noriaki Arakawa
National Institute of Health Science
Atsuhito Ushiki
Shinshu University School of Medicine
Mitsuhiro Abe
Graduate School of Medicine, Chiba University
Shinichiro Matsuyama
National Institute of Health Sciences
Yoshinobu Saito
Graduate School of Medicine, Nippon Medical School
Takeru Kashiwada
Graduate School of Medicine, Nippon Medical School
Yasushi Horimasu
Hiroshima University Hospital
Akihiko Gemma
Graduate School of Medicine, Nippon Medical School
Koichiro Tatsumi
Graduate School of Medicine, Chiba University
Noboru Hattori
Hiroshima University
Kenji Tsushima
International University of Health and Welfare
Kosuke Saito
National Institute of Health Sciences https://orcid.org/0000-0002-1035-3454
Ryosuke Nakamura
National Institute of Health Sciences
Takeshi Toyoda
National Institute of Health Sciences
Kumiko Ogawa
National Institute of Health Sciences
Motonobu Sato
Astellas Pharma Inc.
Kazuhiko Takamatsu

Astellas Pharma Inc.
Kazuhiko Mori
Daiichi Sankyo Co.,Ltd
Takayoshi Nishiya
Daiichi Sankyo RD Novare Co.,Ltd
Takashi Izumi
Kihara Memorial Foundation
Yasuo Ohno
Kihara Memorial Foundation
Yoshiro Saito (yoshiro@nihs.go.jp)
National Institute of Health Sciences
Masayuki Hanaoka
Shinshu University School of Medicine

Article

Keywords: Drug-induced Interstitial Lung Disease, Proteomic Analysis, Bacterial Pneumonia, Bronchoalveolar Lavage Fluid, p53 Activation

Posted Date: July 14th, 2021

DOI: https://doi.org/10.21203/rs.3.rs-690487/v1

Version of Record: A version of this preprint was published at Nature Communications on October 4th, 2022. See the published version at https://doi.org/10.1038/s41467-022-33160-9.

Abstract

Among the various histopathological patterns of drug-induced interstitial lung disease (DILD), diffuse alveolar damage (DAD) is associated with poor prognosis. However, there is no reliable biomarker for its accurate diagnosis. Here, we show stratifin/14-3-3σ (SFN) as a biomarker candidate found in a proteomic analysis. The study included two independent cohorts and controls (n = 432 samples). SFN was specifically elevated in DILD patients with DAD, and was superior to the known biomarkers, KL-6 and SP-D, in discrimination of DILD patients with DAD from patients with other DILD patterns or other lung diseases, including bacterial pneumonia. SFN was also increased in serum from patients with idiopathic DAD, and in lung tissues and bronchoalveolar lavage fluid of patients with DAD. In vitro analysis using the A549 cell line suggested that extracellular release of SFN occurred via p53 activation. We conclude that serum SFN is a promising biomarker for DAD diagnosis.

Introduction

Pharmaceutical products can cause lung injury as an adverse drug reaction; drug-induced interstitial lung disease (DILD) is a common example. In fact, studies have found that epidermal growth factor receptor tyrosine kinase inhibitors (EGFR-TKIs) such as gefitinib and erlotinib frequently cause DILD[1–3]. Although DILD is a problem in Europe and the US (with an incidence of 0.3% for gefitinib), the incidence rate of DILD is higher in Japan (2–3% for gefitinib)[4–7]. The high incidence rate in Japan is considered a serious issue not only in the clinical setting, but also in the context of global drug development.

There are several types of DILD, categorized based on histological patterns. The most serious type is diffuse alveolar damage (DAD). Of note, DAD is frequently observed in patients who have developed DILD due to the administration of tyrosine kinase inhibitors (TKIs), including EGFR-TKIs[8], and is also a common characteristic among the majority of patients with acute lung injury, such as cases of acute exacerbation (AE) of idiopathic pulmonary fibrosis (IPF) and acute respiratory distress syndrome (ARDS). Importantly, patients with DAD do not sufficiently respond to treatment, and their prognosis is poor; additionally, even if they recover from the disease, they continue to suffer from fibrosis. Therefore, for the diagnosis of DILD, early identification of patients with DAD is necessary in order to select an appropriate treatment and avoid severe outcomes or DILD-related death.

Biopsy for pathological evaluation is needed for the definitive diagnosis of DILD, but it is clinically and ethically difficult to obtain samples from patients with DAD because of their severe symptoms. Currently, high-resolution computed tomography (HRCT) chest scans are the most effective non-invasive method to diagnose the histological pattern of DILD[9]. However, it is difficult for general physicians other than respiratory specialists to correctly diagnose DAD by HRCT, because this method requires specialized knowledge and training. In addition, HRCT is highly expensive and poses a significant financial burden on health-care systems. Moreover, exposure to radiation during HRCT scanning is associated with an increase in the long-term risk of complications. Therefore, it is necessary to develop a biomarker that can be used specifically for the diagnosis of DAD.

Currently, the following biomarkers are used in the clinical detection of interstitial pneumonia: surface protein (SP)-A, SP-D, and Krebs von den Lungen-6 (KL-6); all of these are high-molecular-weight glycoproteins that are expressed by type II pneumocytes[10,11]. KL-6 has been reported to be useful for the detection of EGFR-TKI-induced DILD in patients with non-small-cell lung carcinoma[12]. However, although these biomarkers can detect interstitial pneumonia in general, they are not used specifically for the diagnosis of DAD. Moreover, there is no correlation between these biomarkers and the severity of lung injury. In addition to DILD, several blood biomarkers have been proposed for the detection of acute lung injury, including acute interstitial pneumonia and ARDS. Such biomarkers include the molecular chaperone HSP47[13], the inflammatory cytokines IL-1β, IL-8, and IL-6; and the inflammatory mediators HMGB1 and LBP[14]. However, none of these biomarkers are currently used in the clinical setting.

In this study, we performed an aptamer-based proteome analysis using blood samples from DILD patients in order to identify a new diagnostic marker of DAD, and we validated the clinical usefulness of the thus-identified marker using two independent cohorts.

Results

Screening and validation of new biomarkers

We performed a sample collection at the acute and recovery phases from consecutively recruited DILD-onset patients exhibiting the DAD pattern, the DAD pattern mixed with other dominant DILD patterns (DAD-mixed patterns), the organizing pneumonia (OP) pattern, the nonspecific interstitial pneumonia (NSIP) pattern, or the hypersensitivity pneumonitis (HP) pattern. To search for biomarkers specific to patients in the DAD group (the DAD and DAD-mixed patterns), we performed a proteomics study by SOMAscan assay in a “Discovery cohort” of patients with DILD who were enrolled in the early phase of this study, and validated the results using a “Validation cohort” consisting of additional enrolled DILD patients. Tolerant controls (who were administered similar drug(s) but exhibited no DILD onset) and various lung disease patients were also analyzed for biomarker evaluation. The clinical characteristics of these cohorts are shown in Table 1 (for age, sex) and Supplementary Table 1 (for laboratory test). The underlying diseases and the suspected causal drugs of DILD in the registered DILD patients were diverse in both Discovery and Validation cohorts (Supplementary Tables 2 and 3).

Table 1
Sample cohorts used in this study: numbers and characteristics.

Group			Pattern	No. of cases (female)	Age (range)	No. of samples (acute/recovery)
Discovery cohort [95]	HV			24 (12)	61 (55–65)	24
	DILD	**DAD group**		**10 (2)**	**71 (56–86)**	**17 (10/7)**
			DAD*	6 (1)	72 (61–86)	11 (6/5)
			DAD-mixed†	4 (1)	70 (56–82)	6 (4/2)
		non-DAD group		**30 (13)**	**61.5 (32–85)**	**54 (30/24)**
			OP	13 (4)	69 (32–85)	22 (13/9)
			NSIP	15 (6)	63 (46–81)	28 (15/13)
			Other‡	2 (1)	61.5 (50–73)	4 (2/2)
Validation cohort [120]	HV			53 (33)	34 (25–64)	53
	DILD	**DAD group**		**16 (3)**	**69 (54–84)**	**23 (16/7)**
			DAD*	11 (3)	70.5 (60–80)	13 (11/2)

HV, healthy volunteer; IIP, idiopathic interstitial pneumonia; CTD, lung disease associated with connective tissue disease; COPD, chronic obstructive pulmonary disease; NTM, nontuberculous mycobacteria; BA, bronchial asthma; infection, bacterial and mycotic pneumonia. Data of the DAD and non-DAD groups are shown in bold.

*DAD: patients diagnosed with a DAD-only pattern or DAD-dominant pattern (examples of diagnosis: DAD > NSIP, DAD > OP).

†DAD-mixed: patients diagnosed with DILD subtypes other than a DAD-dominant pattern, but in whom co-presence of the DAD pattern was observed by HRCT (examples of diagnosis: OP > DAD, HP > DAD, DAD = HP).

‡Other: cases including eosinophilic pneumonia (EP) and hypersensitivity pneumonitis (HP). OP: organizing pneumonia; NSIP: nonspecific interstitial pneumonia.

Group		Pattern	No. of cases (female)	Age (range)	No. of samples (acute/recovery)
		DAD-mixed†	5 (0)	67 (54–84)	10 (5/5)
	non-DAD group		**28 (15)**	**72.5 (52–79)**	**44 (28/16)**
		OP	17 (11)	72 (52–79)	28 (17/11)
		NSIP	7 (2)	73 (63–77)	10 (7/3)
		Other‡	4 (2)	71.5 (56–75)	6 (4/2)
Tolerant controls [31]	Tolerant controls		31 (12)	69 (33–83)	31
Disease controls [186]	Lung cancer		58 (17)	72 (44–81)	58
	Infectious		19 (3)	75 (36–81)	19
	NTM		14 (9)	65.5 (51–81)	14
	IIPs		43 (8)	72 (41–83)	43
	CTD		25 (16)	67 (50–83)	25
	COPD		15 (2)	67 (51–80)	15

HV, healthy volunteer; IIP, idiopathic interstitial pneumonia; CTD, lung disease associated with connective tissue disease; COPD, chronic obstructive pulmonary disease; NTM, nontuberculous mycobacteria; BA, bronchial asthma; infection, bacterial and mycotic pneumonia. Data of the DAD and non-DAD groups are shown in bold.

*DAD: patients diagnosed with a DAD-only pattern or DAD-dominant pattern (examples of diagnosis: DAD > NSIP, DAD > OP).

†DAD-mixed: patients diagnosed with DILD subtypes other than a DAD-dominant pattern, but in whom co-presence of the DAD pattern was observed by HRCT (examples of diagnosis: OP > DAD, HP > DAD, DAD = HP).

‡Other: cases including eosinophilic pneumonia (EP) and hypersensitivity pneumonitis (HP). OP: organizing pneumonia; NSIP: nonspecific interstitial pneumonia.

Group	Pattern	No. of cases (female)	Age (range)	No. of samples (acute/recovery)
	BA	12 (9)	60 (43–87)	12
HV, healthy volunteer; IIP, idiopathic interstitial pneumonia; CTD, lung disease associated with connective tissue disease; COPD, chronic obstructive pulmonary disease; NTM, nontuberculous mycobacteria; BA, bronchial asthma; infection, bacterial and mycotic pneumonia. Data of the DAD and non-DAD groups are shown in bold.				
*DAD: patients diagnosed with a DAD-only pattern or DAD-dominant pattern (examples of diagnosis: DAD > NSIP, DAD > OP).				
†DAD-mixed: patients diagnosed with DILD subtypes other than a DAD-dominant pattern, but in whom co-presence of the DAD pattern was observed by HRCT (examples of diagnosis: OP > DAD, HP > DAD, DAD = HP).				
‡Other: cases including eosinophilic pneumonia (EP) and hypersensitivity pneumonitis (HP). OP: organizing pneumonia; NSIP: nonspecific interstitial pneumonia.				

First, we performed a SOMAscan assay-based proteomic analysis using plasma samples collected from subjects in the Discovery cohort. Using the quantitative data on 1,310 proteins, we searched for proteins whose expression was particularly changed in the DAD group, *i.e.*, proteins that were increased (fold change (FC) > 2) or decreased (FC < 0.5) in acute-phase patients with DAD versus the control group (healthy volunteers and patients in recovery). A total of 55 proteins met these criteria (listed in Supplementary Table 4). Next, we focused our analyses on the following 8 proteins, due to their high effect size ($g \geq 1.9$) in the group of patients with acute DAD: the upregulated macrophage-capping protein (CAPG), C-C motif chemokine 18 (PARC), stratifin/14-3-3σ (SFN), interleukin-1 receptor antagonist (IL-1Ra) and secreted phospholipase A2 (sPLA2), and the down-regulated carbonic anhydrase 6 (CA6), kallistatin (KAL), and apolipoprotein AI (Apo-AI) (Supplementary Table 5). Among these candidates, SFN caught our attention because its levels were markedly increased in the DAD group (FC: 2.3-fold, $g = 1.9$), and did not change in patients with the OP and NSIP patterns (FC: 1.0 and 1.2, respectively; g values = 0.1 and 0.6, respectively; Supplementary Table 5). Therefore, we next developed an in-house ELISA for SFN to validate the SOMAscan results. As shown in Supplementary Table 6, the results indicated that the analytical performance of SFN ELISA was sufficient to warrant further evaluation of this protein. In a parallel analysis using commercial kits, we measured the levels of sPLA2, PARC, IL-1Ra, Apo-AI, KAL, and KL-6 and SP-D, which are known to be representative biomarkers of interstitial pneumonia, to evaluate their diagnostic performance as DAD-specific biomarkers. Both the results of the assay by ELISA and the results using the commercial kits aligned with the SOMAscan data, except for IL-1Ra (data not shown; no replication of SOMAscan data by ELISA). As expected, the levels of SFN (Fig. 1) and all other candidates (Supplementary Fig. 1) were changed in acute DILD patients compared to healthy volunteers, and returned to levels close to those in healthy volunteers in the recovery phases. Importantly, unlike the levels of KL-6 and SP-D, which were elevated not only in the DAD group but also in the non-DAD group (Fig. 1d

and f), the SFN levels were significantly higher in the DAD group than the non-DAD group ($p < 0.0001$, Fig. 1b).

Next, we validated these findings by measuring these biomarker candidates in DILD patients and healthy volunteers in the Validation cohort. Importantly, the concentrations of each biomarker candidate in DILD patients in the Validation cohort were similar to those obtained in the Discovery cohort (Fig. 1 and Table 2 show the results for SFN, KL-6 and SPD; Supplementary Fig. 1 and Supplementary Table 7 show results for the other candidates). Based on the receiver operating characteristic (ROC) curve analysis, the area under curve (AUC) values obtained with the Discovery cohort were reproduced in the Validation cohort (Fig. 1h and Supplementary Fig. 1m). The AUC values observed in the Validation cohort indicated that all the candidates, except for PARC and Apo-AI, had an extremely good performance (AUC > 0.98) for the discrimination between healthy volunteers and the DAD group. However, in terms of the determination of disease activity in patients with DAD (DAD group patients in the acute phase *versus* all DILD patients in the recovery phase), SFN (AUC [95%CI]: 0.93 [0.84-1.0]) was superior to KL-6 (0.65 [0.48–0.82], SP-D (0.84 [0.71–0.97]) (Fig. 1h), KAL (0.90 [0.81-1.0]) and other candidates (around 0.80) (Supplementary Fig. 1m). In addition, SFN (0.85 [0.73–0.97]) showed the highest DAD-diagnostic performance (discrimination between the DAD group and the non-DAD groups) among these candidates.

Table 2
Comparison of the serum levels of SFN, KL-6, and SP-D in the Discovery and Validation cohorts.

			Concentration median (range), [n]		
			SFN	**KL-6**	**SP-D**
Measurement		Min. Dilution	2-Fold	51-Fold	11-Fold
		LLoQ (unit)	0.1 (ng/mL)	10.0 (U/mL)	17.2 (ng/mL)
HV		Discovery	0.3 (0.1–0.6)	198.6 (114.2–408.0)	51.0 (20.2–164.2)
		Validation	0.2 (0.1–1.9)	162.7 (105.1–391.7)	44.7 (8.6–118.4)
DILD acute	DAD	Discovery	10.0 (3.9–48.3)	1128 (512.0–2018)	278.1 (140.1–1072)
		Validation	8.5 (2.1–34.4)	1136 (316.2–5366)	320.9 (82.7–828.4)
	DAD-mixed	Discovery	8.4 (1.5–20.5)	762.2 (482.5–1019)	281.6 (220.7–635.1)
		Validation	7.9 (3.9–11.4)	417.7 (334.1–1784)	141.3 (70.5–214.4)
	OP	Discovery	0.9 (0.3–2.8)	538.6 (164.2–2408)	128.1 (38.2–765.4)
		Validation	2.3 (0.1–24.1)	1436 (150.5–4217)	231.2 (24.6–1908)
	NSIP	Discovery	2.3 (0.7–7.5)	904.2 (229.0–6826)	187.7 (8.6–1463)
		Validation	1.2 (0.1–43.9)	831.3 (203.0–1156)	168.4 (74.6–445.0)
	Other	Discovery	3.4 (1.8–5.1)	311.6 (273.4–349.9)	130.6 (72.4–188.7)
		Validation	2.6 (0.3–11.5)	408.8 (228.5–532.4)	180.4 (56.2–443.8)
DILD recovery	All	Discovery	0.8 (0.1–87.0)	536.0 (112.7–18959)	105.4 (8.6–436.7)

The matrix used, the minimum dilution factors, the lower limits of quantification (LLoQ), and the concentration of each biomarker in healthy volunteers and DILD patients (median and range), as well as the number of samples measured (n) in the Discovery and Validation cohorts are indicated. DAD, diffuse alveolar damage; OP, organizing pneumonia; NSIP, nonspecific interstitial pneumonia.

	Concentration median (range), [n]		
	SFN	KL-6	SP-D
Validation	0.8 (0.1–12.5)	471.2 (149.4–4474)	93.1 (8.6–428.8)

The matrix used, the minimum dilution factors, the lower limits of quantification (LLoQ), and the concentration of each biomarker in healthy volunteers and DILD patients (median and range), as well as the number of samples measured (n) in the Discovery and Validation cohorts are indicated. DAD, diffuse alveolar damage; OP, organizing pneumonia; NSIP, nonspecific interstitial pneumonia.

Comparison of disease specificity in the Combined sample cohort

Figure 2 shows the distribution of the levels of SFN, and SP-D, and KL-6 in the Combined sample cohort (with combined data from the Discovery and Validation cohorts, and controls). The corresponding values are shown in Supplementary Table 8. The levels of SP-D and KL-6 were elevated not only in the acute phase in all types of DILD patients but also in patients with idiopathic interstitial pneumonias (IIPs) and lung diseases associated with connective tissue diseases (CTDs) (Fig. 2a, b). In contrast, the SFN levels were markedly elevated in a specific fashion in patients with the DAD and DAD-mixed patterns when compared those in the DILD patients with the non-DAD pattern, the tolerant controls or the 7 disease controls ($p < 0.0001$), although infrequent increases of SFN levels were observed in the non-DAD patients of the DILD group, patients with lung carcinoma and IIPs (Fig. 2c). A high level of SFN was not observed in patients with CTDs or infectious lung pneumonia, which are important diseases to discriminate from DILD ($p < 0.0001$, Fig. 2c). Meanwhile, the levels of sPLA2, PARC and KAL were changed in patients with infectious pneumonia, and the level of Apo-AI was dispersed within each patient group (Supplementary Fig. 2; the corresponding values are shown in supplementary Table 8). Thus, for all of these protein candidates, the serum SFN level showed relatively specific association with DAD.

Comparison of the biomarker performance in the Combined cohort

Next, following on the above-described results, we performed a ROC analysis to precisely compare the biomarker performance of SFN to that of the known biomarkers in the Combined cohort (Fig. 3). In terms of the determination of disease activity (acute *versus* recovery patients) in the DAD group, the performance of SFN (AUC [95%CI] 0.93 [0.88–0.99]) was higher than the performances of SP-D (0.86 [0.78–0.95]) and KL-6 (0.68 [0.56–0.80]) (Fig. 3a). Moreover, in terms of the diagnostic performance for discriminating the DAD group from the non-DAD group, SFN (0.90 [0.83–0.97]) was superior to SP-D and KL-6 (AUC $\leq$ 0.61, Fig. 3b). Additionally, the discriminating performance of SFN (0.92 [0.83–1.0]) between the DAD group and tolerant control group (no DILD onset) was almost equivalent to that of SP-D (0.95 [0.89–1.0]), Fig. 3c).

Importantly, the differential diagnosis of DILD depends on the exclusion of infectious pneumonia. Therefore, we also determined the diagnostic performance in this context. Again, SFN was the biomarker showing the strongest performance for discriminating between the acute phase of the DAD group and patients with fungal/bacterial pneumonia (0.98 [0.95–1.0]); the performance of SFN was superior to those of SP-D (0.87 [0.76–0.98]) and KL-6 (0.86 [0.74–0.98]) (Fig. 3d).

Next, we deepened our analysis and focused on the positivity rates; Table 3 shows a comparison of the positivity rates obtained with SFN, SP-D, and KL-6 in various lung diseases. For KL-6 and SP-D, the normal reference levels used in the clinical settings were set as cut-off values (500 U/mL and 110 ng/mL, respectively). For SFN, we applied the Youden Index-based cutoff value of 3.6 ng/mL for discriminating between the DAD group and the tolerant control group. Note that although the Combined cohort data (Fig. 3c) were used to calculate the cutoff value, the Discovery cohort and Validation cohort separately yielded values close to 3.6 ng/mL, indicating the robustness of the cutoff value. Remarkably, none of the healthy volunteers tested positive for SFN, while a high SFN-positivity rate (92%) was observed in the acute-phase patients of the DAD group; meanwhile, the SFN-positivity rates were low in patients with the non-DAD pattern of DILD (10–33%), suggesting that serum SFN-based diagnosis of DAD is possible by setting an appropriate cut-off value for SFN. In addition, the positivity rates of SFN in the DILD patients in recovery, tolerant control patients (mostly lung cancer patients), and lung cancer patients (9%, 10%, and 19%, respectively) were lower than those for KL-6 (50%, 29%, 29%, respectively) and SP-D (44%, 29%, and 26%, respectively). Finally, in patients with infectious pneumonia (n = 19), while 4 and 6 patients were positive for KL-6 and SP-D, respectively, only 1 patient (pneumocystis pneumonia) was positive for SFN. Thus, SFN was found to have a good performance as a DAD-specific biomarker.

Table 3
Comparison of the positivity rates for SFN, KL-6, and SP-D in patients with DILD and three types of controls.

Patient group		%. Positivity rate (N, positive / N, analyzed)		
		SFN	**KL-6**	**SP-D**
	Positive	> 3.6 ng/mL	> 500 U/mL	> 110 ng/mL
HV		0 (0/77)	0 (0/77)	4 (3/77)
DILD acute	**DAD group**	**92 (24/26)**	**81 (21/26)**	**92 (24/26)**
	DAD	94 (16/17)	94 (16/17)	94 (16/17)
	DAD-mixed	89 (8/9)	56 (5/9)	89 (8/9)
	non-DAD group	**17 (10/58)**	**67 (39/58)**	**74 (43/58)**
	OP	10 (3/30)	70 (21/30)	70 (21/30)
	NSIP	23 (5/22)	73 (16/22)	86 (19/22)
	Other	33 (2/6)	33 (2/6)	50 (3/6)
DILD recovery	All	9 (5/54)	50 (27/54)	44 (24/54)
Tolerant control		10 (3/31)	29 (9/31)	29 (9/31)
Lung cancer		19 (11/58)	29 (17/58)	26 (15/58)
Infectious		5 (1/19)	21 (4/19)	32 (6/19)
NTM		7 (1/14)	21 (3/14)	50 (7/14)
IIPs		16 (7/43)	86 (37/43)	88 (38/43)
CTD		8 (2/25)	76 (19/25)	52 (13/25)
COPD		13 (2/15)	40 (6/15)	40 (6/15)
BA		0 (0/12)	0 (0/12)	0 (0/12)

The reference values used in the clinical settings (500 U/mL and 110 ng/mL) were used as the cut-off for KL-6 and SP-D. The Youden's index-based cutoff of 3.6 ng/mL for SFN was obtained by comparing SNF levels in the DAD group and the tolerant control group. Data of the DAD and non-DAD groups are shown in bold. DAD: diffuse alveolar damage; OP: organizing pneumonia; NSIP: nonspecific interstitial pneumonia; IIP: idiopathic interstitial pneumonia; CTD: lung disease associated with connective tissue disease; COPD: chronic obstructive pulmonary disease; NTM: nontuberculous mycobacteria; BA: bronchial asthma; infectious: bacterial and mycotic pneumonia.

SFN levels were not associated with the underlying diseases or causative medications

As previously mentioned, the DILD patients enrolled in this study had various underlying diseases and had been administered several drugs suspected to be the cause of their DILD. The underlying diseases of the DILD patients were classified into three disease groups: lung cancer, other tissue cancer (including pancreatic, esophageal, and breast cancers), and non-cancerous diseases (including heart failure and rheumatoid arthritis) (Supplementary Table 2). The suspected drugs were categorized into the following five types in accordance with their mechanism of action (Supplementary Table 3): DNA-damaging agents (DDAs, including platinum drugs, gemcitabine, irinotecan, bleomycin, and 5-fluorouracil); taxanes (paclitaxel and docetaxel); tyrosine kinase inhibitors (including EGFR-TKIs such as erlotinib and osimertinib, as well as VEGF inhibitors such as axitinib and bevacizumab); immune checkpoint inhibitors (ICIs, including nivolumab, and pembrolizumab); and other drugs (mTOR inhibitors and non-oncology drugs such as antibiotics, anti-rheumatoid drugs, antiarrhythmic agents, and Chinese herbal medicines). In the DAD group, there were no significant differences in the levels of SFN among patients with lung cancer, other tissue cancers, and non-cancerous diseases, and no significant differences among patients treated with the different classes of suspected drugs (Supplementary Fig. 3a and d); in fact, the SFN-positivity rates (> 3.6 ng/mL) were almost equivalent among the groups (Supplementary Tables 10 and 11). In addition, in the non-DAD group and tolerant control patients, no clear relationships were observed between the levels of SFN and underlying diseases or causative drugs (Supplementary Fig. 3b, c, e and f). Collectively, these findings suggest that the increase in the serum levels of SFN in patients with DAD was not affected by the patients' underlying diseases or the administration of any drugs.

Changes in the biomarkers in AE-IIPs

Among the 43 patients with IIPs analyzed (Fig. 2), AE-IIPs were observed in 6 patients (5 with AE-IPF and 1 with acute interstitial pneumonia). In general, DAD is also a histopathologic hallmark of AE-IIPs[17]. Figure 4 shows the distribution of the blood levels of SFN and the two known biomarkers according to the categorization of patients with IIPs. While there was a tendency for the levels of KL-6 and SP-D to be higher in the patients with AE-IIPs, the levels of these biomarkers were also frequently higher (SP-D > 110 ng/mL, KL-6 > 500 U/mL) in patients with IPF and NSIP (Fig. 4b and c). In contrast, the levels of SFN were significantly higher in patients with AE-IIPs compared to patients with the other disease types, who were mostly negative for SFN (< 3.6 ng/mL, Fig. 4a). Therefore, our data suggest that SFN is strongly associated with DAD, and may also be a useful marker for AE-IIPs.

Origin of SFN

To clarify whether the increase of serum SFN levels in patients with DAD was a result of the release of SFN from the damaged lung tissues, we investigated the expression of SFN in lung tissues and bronchoalveolar lavage fluid (BALF) from patients with DAD. We immunohistochemically analyzed 19 lung tissue specimens, including 9 DAD autopsy specimens (from patients with DILD and with AE-IIPs such as ARDS) and 10 control tissues (5 autopsy and 5 surgical specimens from patients with lung cancer). Among the 9 DAD cases, only 1 was negative (−) for SFN expression, 2 had occasional slightly positive cells (±), 2 had some positive lesions (+), and 4 cases had several positive lesions (++). In

contrast, among 10 control specimens, 6 were −, 2 were ±, 1 was + and 1 was ++. Cytoplasmic staining was observed mostly in the basal cells of the bronchioles (Fig. 5a-1) and some alveolar type II cells (Fig. 5a-2). Positive staining was observed in the cells that tended to show type II pneumocyte hyperplasia or squamous cell metaplasia, the pathological features of advanced DAD. The strength of expression was associated with the grade of lesions observed. In contrast, SFN expression was not observed in the cells of alveolitis with bleeding in the lung cancer case (Fig. 5a-3) or in the normal-looking alveolar cells (Fig. 5a-4) of controls. In the non-tumor specimens from the lung cancer patients, a few positive cells were observed in the basal cells of the bronchioles where focal interstitial inflammation was observed.

In addition, significant correlation was observed between the levels of SFN in serum and BALF, which were taken from patients with DILD or IIPs (n = 14, Spearman's rank correlation coefficient [r_s] = 0.670, p = 0.0053) (Fig. 5b). Moreover, there was also a significant correlation between the serum levels of SFN and the PaO_2/FiO_2 ratio, an indicator of blood oxygenation, in DILD patients (n = 40, r_s = − 0.439, p = 0.0023) (Fig. 5c). These results suggest that SFN may be upregulated in damaged cells at the alveoli and bronchioles, and then released into the blood. This finding is supported by the significant correlations observed between the serum SFN levels and the SpO_2/FiO_2 ratio (r_s = − 0.434, p < 0.0001), as well as between the serum levels of SFN and the serum levels of C-reactive protein (CRP) (r_s = 0.520, p < 0.0001) and lactate dehydrogenase (LDH) (r_s = 0.437, p < 0.0001), which are indicators of inflammation and tissue injury, respectively (Supplementary Fig. 4).

Upregulation of SFN in vitro

To elucidate whether lung epithelial cells have the potential to release SFN, the expression of SFN was analyzed *in vitro* using the A549 cell line (derived from type II pneumocytes with an intact p53 gene). Because SFN is known to be a transcription target of p53[18], we examined the expression of SFN in A549 cells treated with a p53-activating reagent (JNJ26854165, which activates p53 via the inhibition of the interaction between p53 and MDM2). Importantly, when A549 cells were treated with various concentrations of JNJ26854165, both the SFN levels and the LDH levels were increased in the conditioned medium, although the decrease in the cell proliferation was found to be dose-dependent (Fig. 6a). In fact, for the A549 cells treated with 10 μg/mL JNJ26854165, while there were slight changes in the amount of intracellularly expressed SFN, the amount of SFN in the conditioned medium was increased by over 500-fold compared to that in the untreated control cells (Fig. 6b). Of note, these results were much more prominent than those obtained with nutlin-3, another p53 activator, and bleomycin and hydrogen peroxide, both associated with ARDS and bleomycin-induced pneumonia[19–21], which exhibited modest increases of over 5-fold (Fig. 6b). The changes in the amount of SFN in the conditioned medium aligned with the results of the mRNA expression of *SFN* (Fig. 6c). We also observed an increase in the expression of the transcription factor p53 and its transcription target p21, indicating the activation of p53 (Fig. 6d). Simultaneously, the levels of extracellularly released LDH and keratin18 (K18) were increased, and in particular, the caspase-cleaved form of K18 (ccK18) was markedly elevated with JNJ26854165, indicating apoptosis induction (Fig. 6e and f). The changes in the extracellular release level and mRNA

level of SFN were similar to that of ccK18. Taken together, these results suggest that SFN may be produced in alveolar epithelial cells in a p53-dependent manner (at least in A549 cells), and immediately released extracellularly via apoptosis.

Discussion

This study sought to identify a blood-based biomarker of DILD and was the first study to evaluate the usefulness of SFN as a DAD marker. In fact, until now, the relationship between SFN and DAD-type interstitial pneumonia has been unclear, and, to the best of our knowledge, no study has reported the detailed behavior of SFN in the blood. In a validation study using our established SFN ELISA, we observed that the serum levels of SFN were specifically increased in patients with DAD. Thus, our findings on SFN were reproduced in samples from an independent cohort. Moreover, the biomarker performance of SFN for discriminating DAD was superior to those of known biomarkers such as KL-6 and SP-D, which are currently used in clinical settings. Additionally, our data suggests that SFN may be useful not only for the diagnosis of drug-induced DAD but also for the diagnosis of idiopathic DAD. We also showed that the levels of SFN were increased not only in the serum, but also in autopsy specimens and the BALF from patients with DAD. Serum SFN levels were significantly correlated with respiratory parameters. In addition, upregulation and extracellular release of SFN were observed in response to the activation of p53 in pulmonary epithelial-derived cells (A549). These findings suggest that serum SFN levels might reflect the degree of lung injury in patients with DAD; thus, this biomarker would be useful for the diagnosis of DILD patients with DAD as well as for the monitoring of their response to treatment.

SFN (14-3-3σ) belongs to the 14-3-3 family, together with six other isoforms, namely β, γ, ε, ζ, η, and τ. This family is a group of highly evolutionarily conserved proteins with a molecular mass of 25–30 kDa, expressed in all eukaryotes and involved in the modulation of various cellular processes via the binding to phosphorylated proteins[22]. While most 14-3-3 isoforms are expressed in various normal tissues in a ubiquitous manner, SFN is expressed specifically in stratified epithelia[23]. In fact, immunohistochemistry staining images of SFN included in the Human Protein Atlas database (https://www.proteinatlas.org) show that SFN is expressed permanently and abundantly in the squamous epithelium of the skin and esophageal tissues; on the other hand, SFN is only very weakly expressed in the normal alveolar epithelium. However, our immunohistochemical analysis using DAD autopsy specimens revealed that SFN was expressed mostly in the basal cells of the bronchioles and some alveolar type II cells that tended to show squamous metaplasia, which is generally observed in the mid to late phase of advanced DAD. Although SFN has been reported to be associated with lung adenocarcinoma[24,25], no such association was observed in the serum samples of our lung cancer patients (Fig. 2 and data not shown). Instead, we would like to emphasize that the marked increase of serum SFN levels occurred specifically in the patients with DAD.

The pathological changes of DAD proceed consistently through discrete but overlapping phases: the early exudative phase, the mid proliferative (organizing) phase, and the late fibrotic phase. They reflect the global mechanisms of wound repair, and are thought to be involved in cell cycle regulation and

apoptosis[26]. Denudation and apoptosis of alveolar epithelia may be important early features of acute lung injury. Guinee et al. reported that the expression of the transcription factor p53 as well as the expression of its transcription targets WAF1 and BAX were increased in type II pneumocytes in the lung of a patient with DAD[27,28]. In addition, Bardales et al. showed that decreases in cell proliferation and increases in apoptosis were frequently observed in the lung tissues of patients with DAD, with both changes tending to be stronger in more severe cases, while apoptosis was undetectable in non-DAD patients[29].

It is also worth noting that SFN is a direct transcriptional target of p53[30]. In the current study, we showed that A549 cells, which were derived from type II alveolar epithelial cells, were able to release SFN *in vitro* via apoptosis in the context of p53 activation (Fig. 6). These findings suggest that SFN may be upregulated by p53 activation when lung epithelial cells are damaged in patients with acute lung injury such as DAD, and extracellularly released via apoptosis, resulting in increased blood SFN levels. In particular, release of SFN into the alveolar epithelium, which is the main field for gas exchange from the lungs to the blood, may contribute significantly to the increase in circulating SFN levels.

There have been many studies on the intracellular function and biological activity of SFN. The expression of SFN has been shown to be induced in a p53-dependent manner in response to DNA damage, and the progression of the G2/M phase of the cell cycle is arrested[30]. In addition, SFN is a marker of the differentiation of epidermal keratinocytes. An analysis based on skin biopsy samples revealed that the expression of SFN in keratinocytes in the squamous epithelium was stronger in areas close to the epidermis; moreover, an experiment using cultured cells found that the upregulation of SFN was closely related to a reduction in cell proliferation and the progression of cellular senescence[23].

Moreover, in addition to intracellular SFN, the role of extracellular released-SFN has also been reported. Previous studies have demonstrated that the expression of SFN increases when keratinocytes are exposed to ultraviolet rays, and that keratinocyte-released SFN affects dermal fibroblasts via paracrine actions, facilitating the expression of matrix metalloproteinase (MMP)-1[31–33]. In addition, in keratinocytes, the extracellular expression of SFN protein is markedly increased compared to the intracellular expression[33], consistent with our data showing that the extracellular SFN levels following p53 activation were much higher than the intracellular levels (Fig. 6b). The above-mentioned studies also suggested that keratinocyte-released SFN may be associated with skin wound healing and suppression of skin fibrosis[31–33]. Based on our results, we believe that the lung epithelia-released SFN may also be associated with pulmonary damage and remodeling. However, the mechanistic link between the increase in SFN in blood and the pathophysiology of DAD requires further study.

DNA-damaging agents (DDAs) such as cisplatin, carboplatin, and bleomycin may potentially activate p53 in cells. However, in this study we observed no significant difference in the serum SFN levels between DILD patients who were administered DDAs and those who were administered other types of drugs (Supplementary Fig. 3). Importantly, these findings show that the measurement of serum SFN can detect

DILD patients with DAD irrespective of the therapeutic agents used, including DDAs. On the other hand, high SFN levels were rarely observed in patients with lung cancer (or other types of cancer) (Table 3 and Supplementary Table 10). Therefore, when using serum SFN for monitoring the onset of DAD in oncology patients undergoing chemotherapy, it may also be necessary to measure the SFN levels prior to drug administration.

Several limitations of this study bear mention. First, although we were able to replicate the current findings, the number of patients enrolled was small. Second, overall, as only the serum levels were examined, the findings of this study do not provide sufficient evidence to indicate a direct relationship between the pathology of DAD and SFN. Indeed, immunohistochemistry data was obtained using autopsy samples from patients with DAD (not from patients assessed for serum SFN levels). Third, high levels of SFN were observed in certain DILD patients with the NSIP or OP pattern, as well as in some lung cancer patients. Therefore, to clarify the reason behind the high levels of SFN in patients without DAD, it is necessary to analyze a larger number of samples. Lastly, this was a retrospective study. Although we demonstrated that SFN increases in patients with DAD, irrespective of either disease types or suspected causative drug types, we cannot completely rule out a potential bias in the selection of patients. Currently, we are collecting serum samples chronologically and prospectively from patients prescribed EGFR-TKI and immune checkpoint inhibitors for future analysis. The analysis of these samples should shed light on the continuous changes in the levels of SFN that accompany the onset of DAD.

In summary, in this study, we identified a protein biomarker for the diagnosis of DAD. SFN showed DAD-specific diagnostic performance, unlike known biomarkers such as KL-6 and SP-D. Since DILD and AE-IIP patients with DAD are likely to have a poor prognosis, it is necessary to make a diagnosis for such patients at the earliest period. Our data suggest that measuring the serum levels of SFN helps to distinguish DAD from other types of DILD, such as OP and NSIP, facilitating the diagnosis of DAD. Therefore, adopting this method may help in the determination of treatment plans for patients with DAD (in addition to the current diagnostic approach based on HRCT findings). Moreover, because SFN is also effective in discriminating the acute phase from the recovery phase, this protein may be useful for monitoring the response to treatment.

Methods

Study population and clinical samples

Clinical samples were collected from the four hub hospitals: Shinshu University, Nippon Medical School, Chiba University, and Hiroshima University. The National Institute of Health Sciences, the Kihara Foundation, Astellas Pharma Inc., and Daiichi Sankyo Company, Ltd. also participated in this study. Approval was obtained from each research ethics review committee and samples were collected in accordance with the approved protocols. Serum and plasma samples were collected from patients who were suspected to have developed drug-induced interstitial pneumonia during the acute (around the most severe phase) and recovery phases of DILD, after informed consent was obtained. DILD was diagnosed

according to the Japanese diagnostic criteria by the respiratory specialists, as follows: 1) history of ingestion of a drug that is known to induce lung injury, 2) appearance of clinical manifestations after drug administration, 3) improvement of clinical manifestations after drug discontinuation, 4) exclusion of other causes of the clinical manifestations, and 5) exacerbation of clinical manifestations after resuming drug administration (challenge testing). Of note, criterion 5) was not used in this study due to ethical issues. Patient recovery was judged by respiratory specialists of each hospital at least two weeks following the onset of DILD, based on recovery of clinical manifestations, improvement of lung imaging findings (e.g., HRCT), and improvement of oxygenation (e.g., SpO_2). Blood samples were collected from patients with any of the following conditions: lung cancer, non-tuberculosis mycobacteriosis, idiopathic interstitial pneumonia (IIP), lung disease associated with connective tissue disease, chronic obstructive pulmonary disease, bronchial asthma, and mycotic/bacterial pneumonia. Blood samples were also collected from tolerant control patients, most of whom were lung cancer patients undergoing chemotherapy without the development of DILD over the course of at least three months. The following tubes were used for blood sampling: Vacutainer (Becton Dickinson, Franklin Lakes, NJ, USA) vacuum blood sampling tubes (6 mL) containing a blood coagulation accelerant for serum collection, and Vacutainer vacuum blood sampling tubes (7 mL) containing EDTA-2Na for plasma collection. The tubes containing the blood were centrifuged for 10 min at 1300 × g, and serum and plasma were divided into small amounts and placed into polypropylene tubes with a screw cap. The samples were then stored in a deep freezer (− 80°C) until they were used.

Samples from healthy volunteers were collected at Yaesu Sakura-Dori Clinic after approval was obtained from the research ethics review committees of the participating organizations. The above-described protocols were followed to obtain serum and plasma samples. The inclusion criteria for healthy volunteers were as follows: (1) Japanese (self-declaration that all family members up to grandparents were Japanese) and diagnosed as healthy by their physician, (2) fasted for at least 14 h before blood collection (only drinking water was permitted), (3) no consumption of any drugs for at least 1 week, and (4) a normal body mass index ($18.5 \leq BMI < 25$). The exclusion criterion was (5) female individuals menstruating.

The “Discovery cohort” consisted of samples from DILD patients in the acute and recovery phases collected from April 2015 to November 2016 and samples from age-matched healthy volunteers. The Discovery cohort was used for biomarker discovery. Thereafter, an independent “Validation cohort” was created, consisting of samples from DILD patients collected from December 2016 to May 2019 and samples from the healthy volunteers that were not included in the Discovery cohort. Importantly, samples from patients with related lung diseases (lung cancer, IIP, lung disease associated with connective tissue disease, chronic obstructive pulmonary disease, nontuberculous mycobacteria, bronchial asthma, and bacterial and mycotic pneumonia) were also included in the Validation cohort for biomarker validation. In some cases, BALF samples collected at Chiba University were also used for analysis. DAD autopsy specimens from patients with interstitial pneumonia, and non-tumor autopsy or surgical specimens from

patients with lung cancer, which were obtained at Shinshu University, were also used for immunohistochemical analysis.

DILD disease classification

Respiratory specialists at each hospital who were extensively experienced in DILD diagnosis classified the histopathological subtypes of DILD (e.g., DAD, OP, and NSIP). The DAD pattern was diagnosed based on the presence of diffuse ground-glass opacities and/or infiltrated shadows in the bilateral lung fields on HRCT. Typical DAD patterns and DAD-dominant patterns (e.g., DAD > HP, DAD > OP) were classified as the DAD pattern. Cases with co-presence of the DAD and non-DAD patterns, but not DAD-dominant (e.g., OP > DAD, HP > DAD, DAD = HP) were classified as the DAD-mixed pattern. Patients with the DAD and DAD-mixed patterns were studied as the DAD-group. In contrast, patients with the OP pattern, NSIP pattern, and HP pattern were categorized as the non-DAD group. Specialists from the four hub hospitals held a meeting and reviewed the patterns based on clinical findings and HRCT images to reach a consensus on their diagnosis.

SOMAscan assay

The SOMAscan system (SomaLogic, Boulder, CO, USA) was used to perform proteomic analyses. Briefly, frozen plasma samples were sent to SomaLogic (Boulder, CO, USA) through the NEC Corp. (Tokyo, Japan). A total of 1,310 proteins were obtained through the SOMAscan assay. For each protein probe, the relative fluorescence units (RFUs) were logarithmically transformed. Thereafter, a control group was set in which data from all recovered patients and healthy volunteers in the Discovery cohort were integrated. A search was performed for proteins whose abundance was significantly different between the DAD group (acute phase, with the DAD or the DAD-mixed patterns) and the control group, based on changes in mean values (fold change: FC), and effect size (Hedge's, *g*).

Measurement of SFN by in-house ELISA

Stratifin/14-3-3 (SFN) was measured using an in-house ELISA kit, which was developed using two commercially available anti-SFN mouse monoclonal antibodies, and recombinant human SFN protein produced in *E. coli* (ATGen, now NKMAX, Seongnam, Korea) as a standard. Briefly, a mouse anti-SFN monoclonal antibody (mAb) used as the primary capture antibody (clone CS112-2A8; Merck, Kenilworth, NJ, USA) was added to Nunc MaxiSorp 96-well microtiter plates (Thermo Fischer Scientific, Waltham, MA, USA) to prepare a solid phase. The plates were washed with a commercial washing buffer (Quantikine Wash Buffer; R&D Systems, Minneapolis, MN, USA) three times at 25°C, and then incubated with the SuperBlock reagent (Thermo Fischer Scientific). The plates were then washed three times at 25°C, and 50 µL samples (serum samples or standard SFN) diluted with General Serum Diluent (Immunochemistry Technologies, Bloomington, MN, USA) were added, followed by 50 µL of the assay buffer (SuperBlock reagent containing 2M KCL and 50 µg/mL of the HBR-1 heterophilic antibody blocking reagent [Scantibodies Laboratory, Santee, CA, USA]), and the plates were stirred for 2 h. Following three washes, the SuperBlock reagent containing biotin-labeled secondary detection antibody (mouse anti-SFN mAb, 3c3; Sigma-Aldrich, St. Louis, MO, USA) was added and incubated for 1 h. After washing six times, plates

were reacted with 10% SuperBlock/PBS solution containing Streptavidin-Poly HRP40 (Stereospecific Detection Technologies, Baesweiler, Germany). SFN was then quantitatively measured using the QuantaRed Enhanced Chemifluorescent HRP Substrate (Thermo Fischer Scientific).

This ELISA assay was validated with reference to the Japanese Guidelines on Bioanalytical Method Validation (Ligand Binding Assay) in Pharmaceutical Development (https://www.pmda.go.jp/files/000206208.pdf). We confirmed that the analytical parameters were sufficient for our current purposes within the criteria of the guidelines (Supplementary Table 2). Moreover, the ELISA method was used to measure SFN concentrations in the cell extracts, conditioned medium, and BALF. SFN concentrations in BALF were normalized with each concentration of urea in BALF and serum according the method of Rennard et al.[34], and then represented as the concentration in epithelial lining fluid (ELF). The urea concentration was determined using a urea nitrogen colorimetric detection kit (Arbor Assays, Ann Arbor, MI, USA).

Commercially available kits

The serum levels of SP-D and KL-6 were measured using in vitro diagnostic kits, SP-D kit YAMASA EIA II (Yamasa, Chiba, Japan) and the E test TOSOH II (Tosoh, Tokyo), respectively. Serum kallistatin (KAL) was measured using DuoSet ELISA, and plasma C-C motif chemokine 18 (PARC) and plasma interleukin-1 receptor antagonist (IL-1Ra) were using Quantikine ELISA kits from R&D Systems (Minneapolis, MN, USA). Secreted phospholipase A2 (sPLA2) and apolipoprotein A-I (apo A-I) in plasma were measured using ELISA kits from Cayman Chemical (Ann Arbor, MI, USA) and Abcam (Cambridge, UK), respectively. All ELISA kits were used in accordance with the manufacturers' instructions.

Immunohistochemistry of SFN

To investigate the expression and localization of SFN in the human lung, immunohistochemical analysis was performed with DAD autopsy specimens from patients with DILD or IIPs, and non-tumor autopsy or surgical specimens from patients with lung cancer. The sections were deparaffinized, hydrated, and then immersed in 3% H_2O_2/methanol solution for 10 min at 25 ºC for inactivation of endogenous peroxidase activity. After blocking nonspecific reactions with 10% normal goat serum, the sections were incubated with a primary antibody targeting SFN (diluted 1:1000; rabbit anti-SFN polyclonal antibody [HPA011105], Atlas Antibodies, Bromma, Sweden) overnight at 4 ºC. Visualization of antibody binding was performed using a VectaStain Elite ABC Kit (Vector Laboratories, Burlingame, CA, USA) and 3,3'-diaminobenzidine. All sections were counterstained with hematoxylin. The strength of staining was scored under a light microscope using the following criteria: −, almost all negative cells; ±, occasional slightly positive cells; +, some apparently positive lesions; ++, several positive lesions for SFN.

In vitro experiments

The A549 cancer cell line derived from human type II pneumocytes was obtained from the JCRB Cell Bank and cultured by the recommended methods. Briefly, the cells were plated in 6-well plates at a density of 1.0×10^5 cells/well. Twenty-four hours later, bleomycin (Cayman Chemical, Ann Arbor, MI, USA),

JNJ26854165 (Cayman Chemical), Nutlin-3a (Selleck Chemicals, Houston, TX, USA), or hydrogen peroxide solution (Nacalai Tesque, Kyoto, Japan) was added to the cells. Forty-eight hours after the addition of the agents, the conditioned medium was collected. Cell extracts were prepared using RIPA buffer (Wako, Richmond, VA, USA). SFN in conditioned medium and cell extracts was measured using the in-house ELISA method. The Viability/Cytotoxicity Multiplex Assay Kit (Dojindo Rockville MD, USA) was used to measure the cell proliferation rate and LDH activity. For Western blotting of p53 and p21, the mAbs mouse anti-p53 (DO-1; Invitrogen, Carlsbad, CA, USA) and rabbit anti-p21 Waf1/Cip1 (12D1; Cell Signaling Technology, Leiden, the Netherlands) were used. The K18 and ccK18 ELISA kits were used for detecting apoptosis.

qRT-PCR analysis

SFN mRNA was measured by real-time PCR. Total RNA was extracted from the cells using RNeasy spin columns (Qiagen, Hilden, Germany). The extracted total RNA was then quantitatively measured using a One Step SYBR PrimeScript RT-PCR Kit (Takara, Kyoto, Japan) and the ABI PRISM 7700 PCR thermal cycler. The β-actin gene (*ACTB*) was used as the internal standard. The PCR primers with the following sequences were used: SFN-F, 5'-TGACGACAAGAAGCGCATCAT; SFN-R, 5'-GTAGTGGAAGACGGAAAAGTTCA; ACTB-F 5'-CACCATTGGCAATGAGCGGTTC; ACTB-R, 5'-AGGTCTTTGCGGATGTCCACGT.

Statistical analysis

The difference in the degree of changes in the amounts of proteins, as per the SOMAscan analysis, was evaluated via the calculation of Hedge's g values. Statistically significant differences between two groups of candidate marker proteins were calculated by the Mann-Whitney U test. The diagnostic performance of each candidate was evaluated based on the AUC values of ROC curves. The cut-off value for SFN was set based on Youden's index in comparison with the DAD group and the tolerant control. Spearman's nonparametric analysis was used to evaluate the correlation between variables. All data were analyzed using the following software: GraphPad PRISM (version 8.4.3; GraphPad Software, San Diego, CA, USA) and Microsoft Excel.

Data Availability

The source data underlying all figures and supplementary figures are provided as a Source Data file.

Declarations

Acknowledgements

We thank Keiko Miyashita for her analytical assistance in the validation of SFN ELISA, and Kazuishi Kubota, Naoya Wada and Kazumi Ito for their technical advice. Financial support was received in the form of grants from the Japan Agency for Medical Research and Development (nos.

19mk01045 and 20mk01073j to YO and YS), and a KAKENHI Grant-in-Aid for Scientific Research (C) from the Ministry of Education, Culture, Sports, Science and Technology of Japan (no. g20K07366 to NA).

Author contributions

Conceptualization: NA, YoshiroS, MH

Data curation: KS, YoshiroS

Methodology: NA, RN, MS, KT, KM, TN, TT, KO, YoshiroS, MH

Investigation: NA, SM, RN, TT

Funding acquisition: NA, KS, AG, KT, NH, YO, YoshiroS, MH

Project administration: TI, YoshiroS, MS, KT, KM, TN, YO

Resources: AU, MA, YoshinobuS, TK, YH, AG, KT, NH, MH

Supervision: YO, YoshiroS, MH

Writing – original draft: NA, KO, YoshiroS.

Writing – review & editing: All authors

Competing interests

NA, RN, MS, TN, YoshiroS and MH are inventors of patents related to biomarker proteins involved in the diagnosis of DILD as filed by the National Institute of Health Science.

References

1. Mok, T. S. *et al.* Gefitinib or carboplatin-paclitaxel in pulmonary adenocarcinoma. *N Engl J Med* **361**, 947–957, doi:10.1056/NEJMoa0810699 (2009).
2. Zhou, C. *et al.* Erlotinib versus chemotherapy as first-line treatment for patients with advanced EGFR mutation-positive non-small-cell lung cancer (OPTIMAL, CTONG-0802): a multicentre, open-label, randomised, phase 3 study. *Lancet Oncol* **12**, 735–742, doi:10.1016/s1470-2045(11)70184-x (2011).
3. Qi, W. X., Sun, Y. J., Shen, Z. & Yao, Y. Risk of interstitial lung disease associated with EGFR-TKIs in advanced non-small-cell lung cancer: a meta-analysis of 24 phase III clinical trials. *J Chemother* **27**,

40–51, doi:10.1179/1973947814y.0000000189 (2015).

4. Cohen, M. H., Williams, G. A., Sridhara, R., Chen, G. & Pazdur, R. FDA drug approval summary: gefitinib (ZD1839) (Iressa) tablets. *Oncologist* **8**, 303–306, doi:10.1634/theoncologist.8-4-303 (2003).
5. Cohen, M. H., Johnson, J. R., Chen, Y. F., Sridhara, R. & Pazdur, R. FDA drug approval summary: erlotinib (Tarceva) tablets. *Oncologist* **10**, 461–466, doi:10.1634/theoncologist.10-7-461 (2005).
6. Ando, M. *et al.* Predictive factors for interstitial lung disease, antitumor response, and survival in non-small-cell lung cancer patients treated with gefitinib. *J Clin Oncol* **24**, 2549–2556, doi:10.1200/jco.2005.04.9866 (2006).
7. Endo, M., Johkoh, T., Kimura, K. & Yamamoto, N. Imaging of gefitinib-related interstitial lung disease: multi-institutional analysis by the West Japan Thoracic Oncology Group. *Lung Cancer* **52**, 135–140, doi:10.1016/j.lungcan.2006.02.002 (2006).
8. Lind, J. S., Smit, E. F., Grünberg, K., Senan, S. & Lagerwaard, F. J. Fatal interstitial lung disease after erlotinib for non-small cell lung cancer. *J Thorac Oncol* **3**, 1050–1053, doi:10.1097/JTO.0b013e318183a9f5 (2008).
9. Silva, C. I. & Müller, N. L. Drug-induced lung diseases: most common reaction patterns and corresponding high-resolution CT manifestations. *Semin Ultrasound CT MR* **27**, 111–116, doi:10.1053/j.sult.2006.01.001 (2006).
10. Ohnishi, H. *et al.* Comparative study of KL-6, surfactant protein-A, surfactant protein-D, and monocyte chemoattractant protein-1 as serum markers for interstitial lung diseases. *Am J Respir Crit Care Med* **165**, 378–381, doi:10.1164/ajrccm.165.3.2107134 (2002).
11. Kinder, B. W. *et al.* Serum surfactant protein-A is a strong predictor of early mortality in idiopathic pulmonary fibrosis. *Chest* **135**, 1557–1563, doi:10.1378/chest.08-2209 (2009).
12. Kawase, S. *et al.* Change in serum KL-6 level from baseline is useful for predicting life-threatening EGFR-TKIs induced interstitial lung disease. *Respir Res* **12**, 97, doi:10.1186/1465-9921-12-97 (2011).
13. Kakugawa, T. *et al.* Serum heat shock protein 47 levels in patients with drug-induced lung disease. *Respir Res* **14**, 133, doi:10.1186/1465-9921-14-133 (2013).
14. Mokra, D. & Kosutova, P. Biomarkers in acute lung injury. *Respir Physiol Neurobiol* **209**, 52–58, doi:10.1016/j.resp.2014.10.006 (2015).
15. Kitsiouli, E., Nakos, G. & Lekka, M. E. Phospholipase A2 subclasses in acute respiratory distress syndrome. *Biochim Biophys Acta* **1792**, 941–953, doi:10.1016/j.bbadis.2009.06.007 (2009).
16. Papiris, S. A. *et al.* High levels of IL-6 and IL-8 characterize early-on idiopathic pulmonary fibrosis acute exacerbations. *Cytokine* **102**, 168–172, doi:10.1016/j.cyto.2017.08.019 (2018).
17. Kaarteenaho, R. & Kinnula, V. L. Diffuse alveolar damage: a common phenomenon in progressive interstitial lung disorders. *Pulm Med* 2011, 531302, doi:10.1155/2011/531302 (2011).
18. Hermeking, H. *et al.* 14-3-3sigma is a p53-regulated inhibitor of G2/M progression. *Mol Cell* **1**, 3–11, doi:10.1016/s1097-2765(00)80002-7 (1997).

19. Xu, X. *et al.* A2BAR activation attenuates acute lung injury by inhibiting alveolar epithelial cell apoptosis both in vivo and in vitro. *Am J Physiol Cell Physiol* **315**, C558-c570, doi:10.1152/ajpcell.00294.2017 (2018).
20. Yan, X. *et al.* Nrf2/Keap1/ARE Signaling Mediated an Antioxidative Protection of Human Placental Mesenchymal Stem Cells of Fetal Origin in Alveolar Epithelial Cells. *Oxid Med Cell Longev* 2019, 2654910, doi:10.1155/2019/2654910 (2019).
21. Wallach-Dayan, S. B. *et al.* Bleomycin initiates apoptosis of lung epithelial cells by ROS but not by Fas/FasL pathway. *Am J Physiol Lung Cell Mol Physiol* **290**, L790-l796, doi:10.1152/ajplung.00300.2004 (2006).
22. Chan, T. A., Hermeking, H., Lengauer, C., Kinzler, K. W. & Vogelstein, B. 14-3-3Sigma is required to prevent mitotic catastrophe after DNA damage. *Nature* **401**, 616–620, doi:10.1038/44188 (1999).
23. Dellambra, E. *et al.* Downregulation of 14-3-3sigma prevents clonal evolution and leads to immortalization of primary human keratinocytes. *J Cell Biol* **149**, 1117–1130, doi:10.1083/jcb.149.5.1117 (2000).
24. Shiba-Ishii, A. *et al.* High expression of stratifin is a universal abnormality during the course of malignant progression of early-stage lung adenocarcinoma. *Int J Cancer* **129**, 2445–2453, doi:10.1002/ijc.25907 (2011).
25. Shiba-Ishii, A. & Noguchi, M. Aberrant stratifin overexpression is regulated by tumor-associated CpG demethylation in lung adenocarcinoma. *Am J Pathol* **180**, 1653–1662, doi:10.1016/j.ajpath.2011.12.014 (2012).
26. Martin, T. R., Nakamura, M. & Matute-Bello, G. The role of apoptosis in acute lung injury. *Crit Care Med* **31**, S184–188, doi:10.1097/01.CCM.0000057841.33876.B1 (2003).
27. Guinee, D., Jr. *et al.* The potential role of BAX and BCL-2 expression in diffuse alveolar damage. *Am J Pathol* **151**, 999–1007 (1997).
28. Guinee, D., Jr. *et al.* Association of p53 and WAF1 expression with apoptosis in diffuse alveolar damage. *Am J Pathol* **149**, 531–538 (1996).
29. Bardales, R. H., Xie, S. S., Schaefer, R. F. & Hsu, S. M. Apoptosis is a major pathway responsible for the resolution of type II pneumocytes in acute lung injury. *Am J Pathol* **149**, 845–852 (1996).
30. Taylor, W. R. & Stark, G. R. Regulation of the G2/M transition by p53. *Oncogene* **20**, 1803–1815, doi:10.1038/sj.onc.1204252 (2001).
31. Ghaffari, A. *et al.* Fibroblast extracellular matrix gene expression in response to keratinocyte-releasable stratifin. *J Cell Biochem* **98**, 383–393, doi:10.1002/jcb.20782 (2006).
32. Medina, A., Ghaffari, A., Kilani, R. T. & Ghahary, A. The role of stratifin in fibroblast-keratinocyte interaction. *Mol Cell Biochem* **305**, 255–264, doi:10.1007/s11010-007-9538-y (2007).
33. Seok, J. K. & Boo, Y. C. p-Coumaric Acid Attenuates UVB-Induced Release of Stratifin from Keratinocytes and Indirectly Regulates Matrix Metalloproteinase 1 Release from Fibroblasts. *Korean J Physiol Pharmacol* **19**, 241–247, doi:10.4196/kjpp.2015.19.3.241 (2015).

34. Rennard, S. I. *et al.* Estimation of volume of epithelial lining fluid recovered by lavage using urea as marker of dilution. *J Appl Physiol (1985)* **60**, 532–538, doi:10.1152/jappl.1986.60.2.532 (1986).

Figures

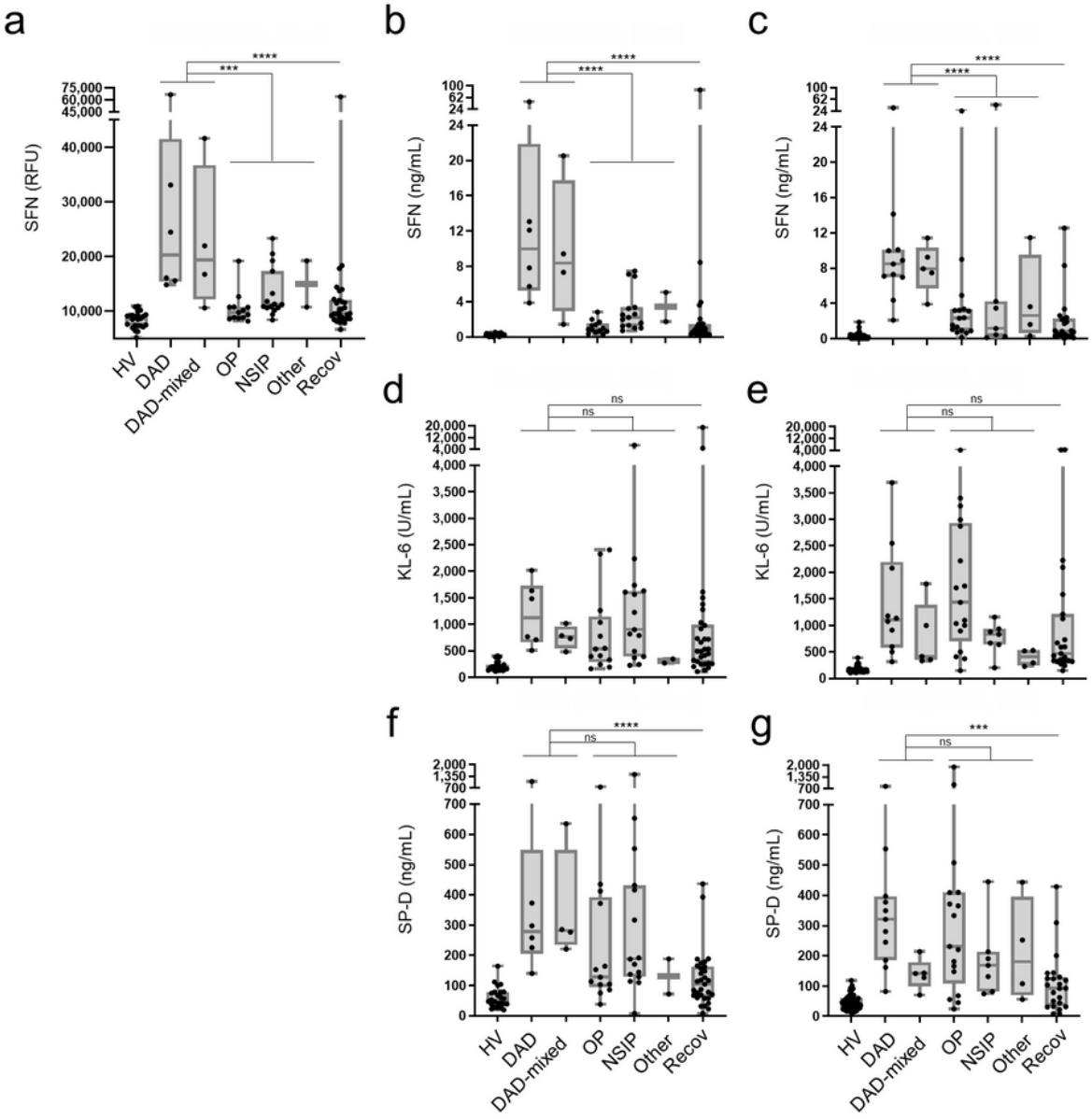

h

		AUC (95% CI)		
		SFN	KL-6	SP-D
DAD group vs HV	Discovery	1.0 (1.0 - 1.0)	1.0 (1.0 - 1.0)	1.0 (0.98 - 1.0)
	Validation	1.0 (1.0 - 1.0)	1.0 (0.99 - 1.0)	0.98 (0.95 - 1.0)
DAD group vs Recovery	Discovery	0.93 (0.85 - 1.0)	0.70 (0.54 - 0.86)	0.92 (0.83 - 1.0)
	Validation	0.93 (0.84 - 1.0)	0.65 (0.48 - 0.82)	0.84 (0.71 - 0.97)
DAD group vs non-DAD	Discovery	0.92 (0.82 - 1.0)	0.59 (0.42 - 0.77)	0.70 (0.54 - 0.86)
	Validation	0.85 (0.73 - 0.97)	0.53 (0.35 - 0.71)	0.54 (0.37 - 0.71)

Figure 1

Blood levels of SFN and known biomarkers for the detection of acute DILD. SOMAscan signals of SFN (a) and serum levels of SFN (b, c), KL-6 (d, e) and SP-D (f, g) measured by ELISA (b-c) or clinical chemistry kits (d-g) in healthy volunteers (HV) and DILD patients in the Discovery (b, d, f) and Validation cohorts (c, e, g) are shown. The boxes indicate interquartile ranges (75% and 25%) and medians. DAD: diffuse alveolar damage; OP: organizing pneumonia; NSIP: nonspecific interstitial pneumonia; Recov: all recovery patients. **p < 0.01; ***p < 0.001; ****p < 0.0001; ns, not significant. h. The area under the curve (AUC) was derived from receiver operating characteristic (ROC) curves, and the 95% confidence intervals (95% CIs) were determined for the biomarkers in comparative analyses.

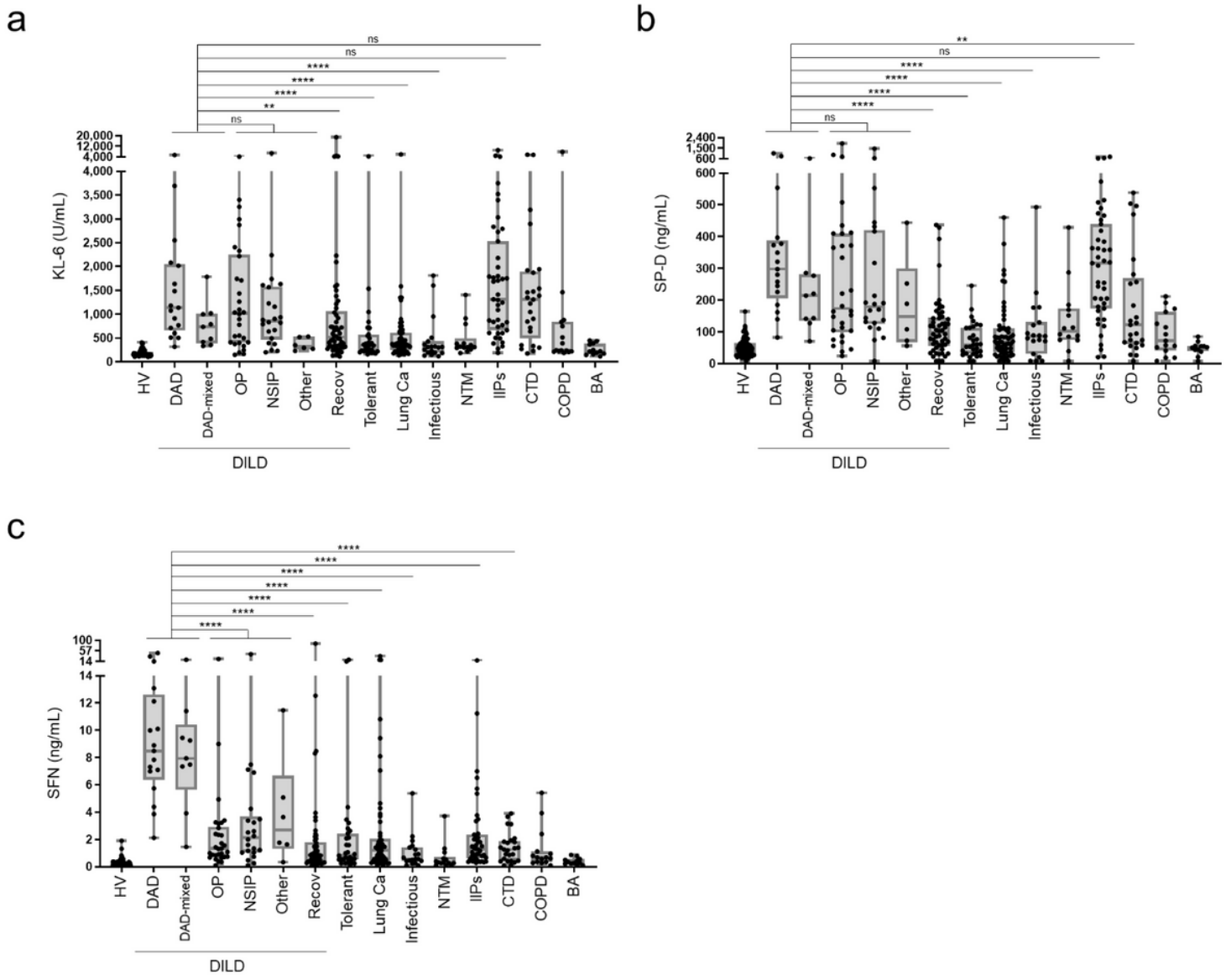

Figure 2

Distribution of SFN and known biomarkers in healthy volunteers and patients with various lung diseases. Results for the Combined cohort are shown. Serum levels of KL-6 (a), SP-D (b), and SFN (e) were measured by ELISA. The boxes indicate interquartile ranges (75% and 25%) and medians. DAD: diffuse alveolar damage; OP: organizing pneumonia; NSIP: nonspecific interstitial pneumonia; Recov: all DILD

patients in recovery; Tolerant: tolerant control; Lung Ca: lung cancer; IIPs: idiopathic interstitial pneumonia; CTD: lung disease associated with connective tissue disease; COPD: chronic obstructive pulmonary disease; NTM: nontuberculous mycobacteria; BA: bronchial asthma; infectious: bacterial and mycotic pneumonia. *p < 0.05, **p < 0.01; ***p < 0.001; ****p < 0.0001; ns, not significant.

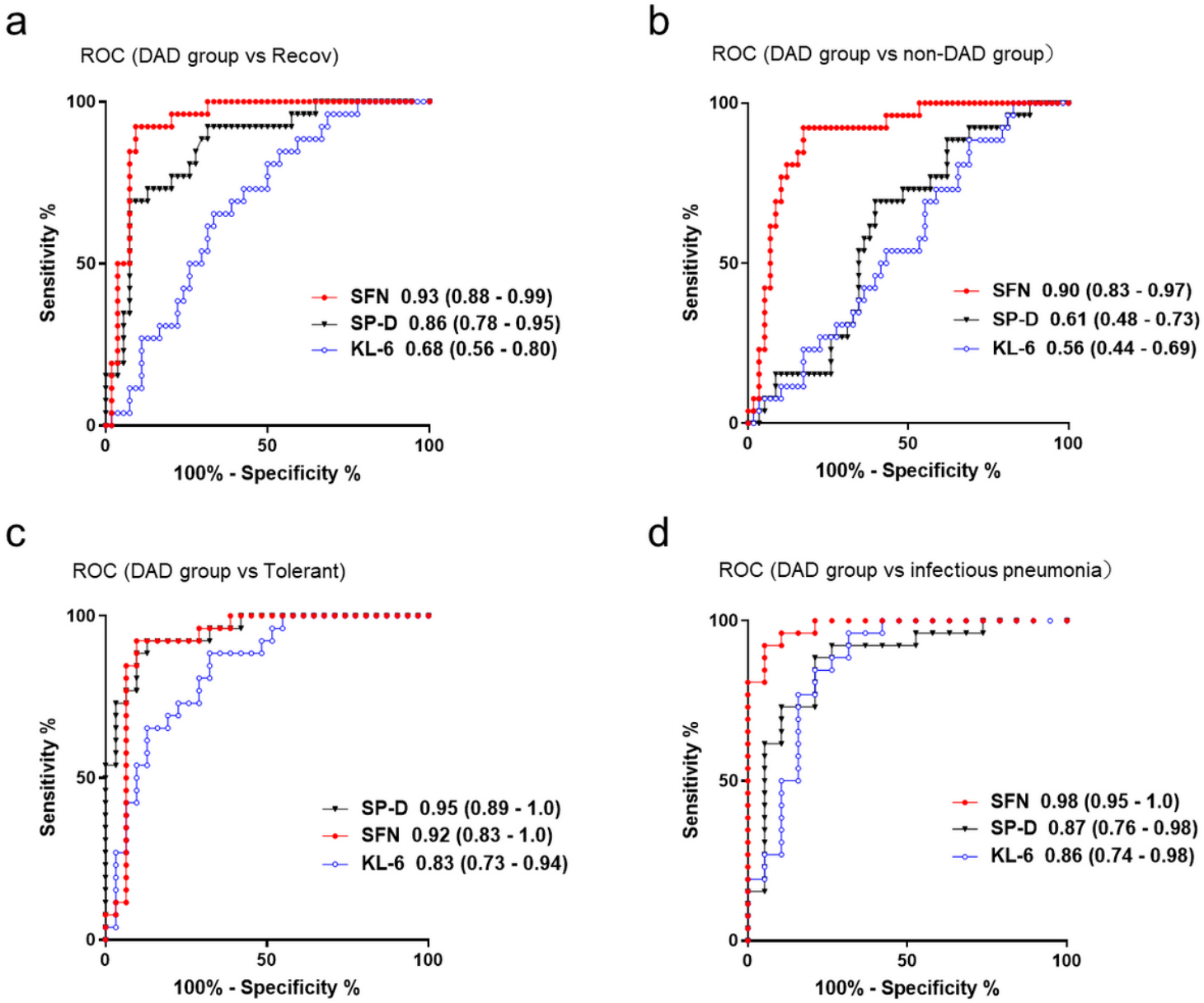

Figure 3

ROC curves for SFN and known biomarkers. Data of the Combined cohort are shown. ROC curves for SFN and KAL as well as the existing markers (SP-D and KL-6) were drawn to discriminate the acute phase of DAD patients from (a) all patients in recovery (discrimination of the disease activity), (b) acute-phase patients with other DILD types (DAD diagnostic performance), (c) the DILD-tolerant control patients (DAD onset), and (d) patients with infectious lung disease. Values in parentheses indicate the area under the curve (AUC) values.

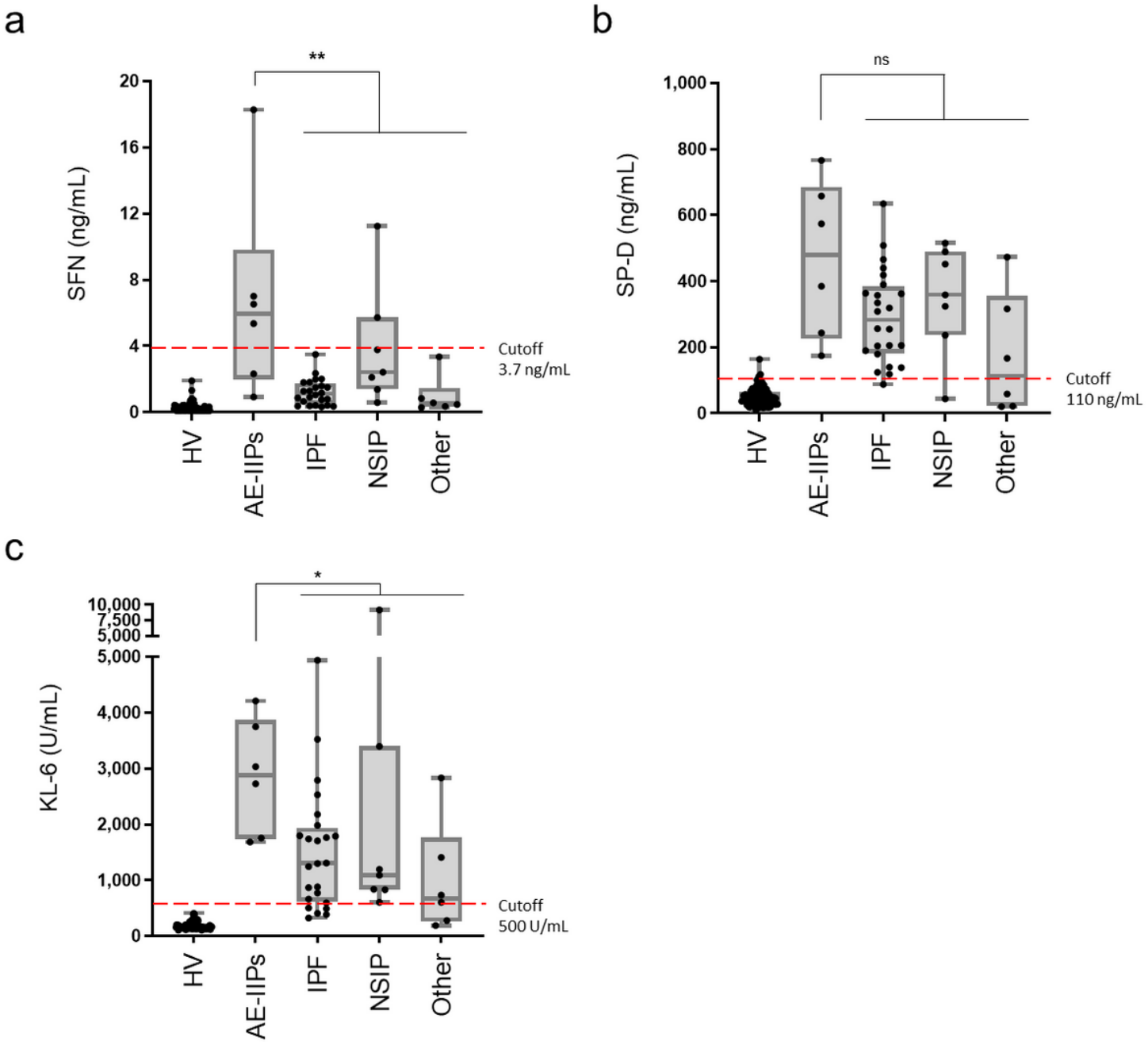

Figure 4

Serum levels of SFN and known biomarkers in idiopathic interstitial pneumonias. The distributions of SFN (a), SP-D (b), and KL-6 (c) are shown in box-plot graphs. The boxes indicate interquartile ranges (75% and 25%) and medians. The broken lines indicate the respective cutoff values. AE-IIPs: Acute exacerbation of idiopathic interstitial pneumonias (DAD-type disease); IPF: idiopathic pulmonary fibrosis; NSIP: nonspecific interstitial pneumonia; Other: other types of idiopathic interstitial pneumonia. *$p < 0.05$; **$p < 0.01$; ns, not significant.

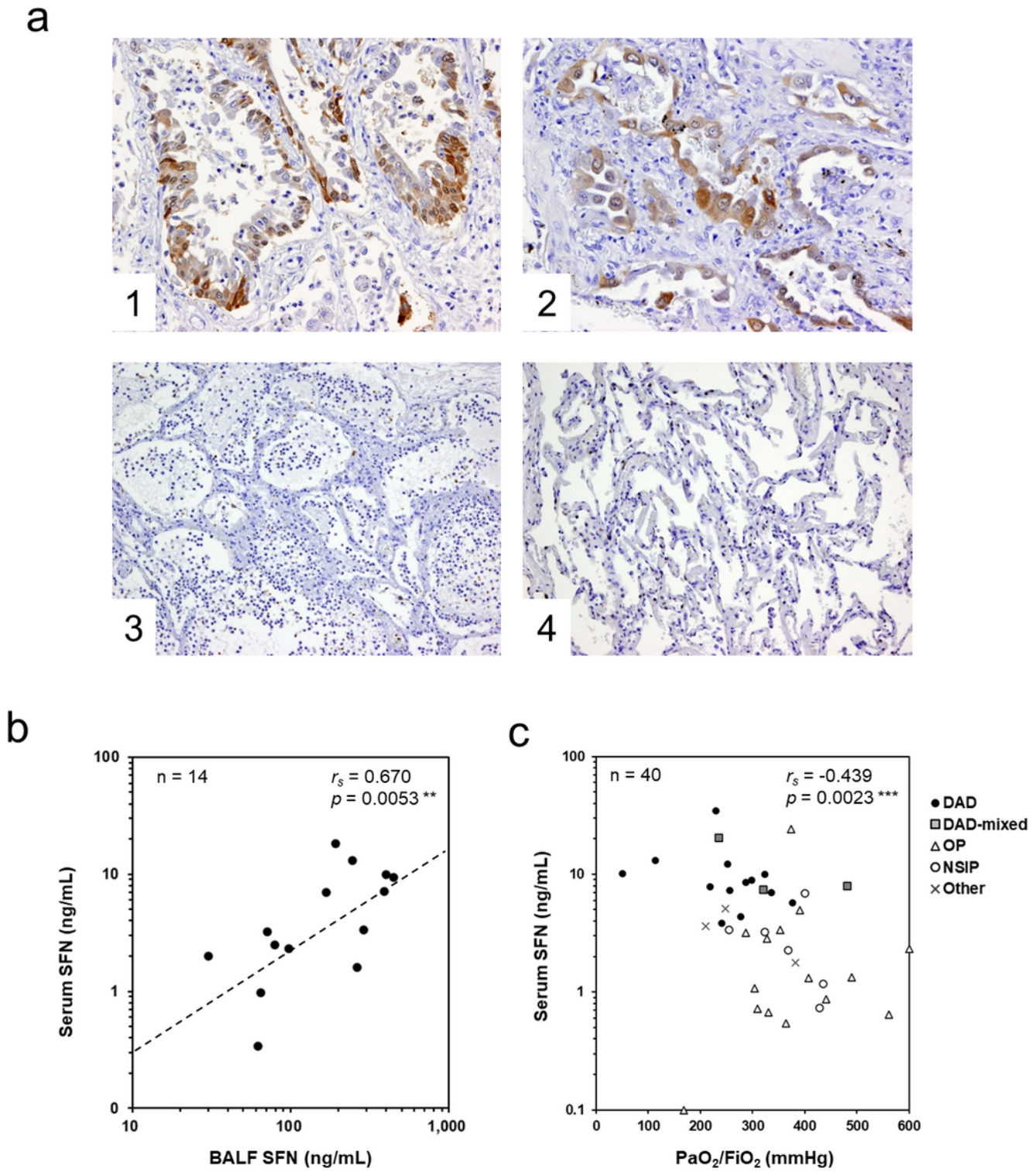

Figure 5

SFN expression in lung tissue, and associations of serum SFN levels with those in BALF and with pulmonary functions. a Representative immunohistochemical staining for SFN. Clear expression was observed in the basal cells of the bronchioles (a1, 200x) and alveolar type II cells (a2, 200x) in DAD specimens. Positive staining was not observed in the cells of alveolitis with bleeding in lung cancer patients (a3, 100x) and normal-looking lung tissue (a4, 100x). b Correlation between serum SFN and

BALF SFN. The data are for patients with DILD or IIPs (n=14) from whom both serum and BALF samples were taken. BALF (ELF) SFN levels were estimated using the urea method. c Correlation between serum SFN levels and the ratio of arterial partial pressure of oxygen to fractional inspired oxygen (PaO2/FiO2) in the acute-phase DILD patients (n=40). The values of the correlation coefficients rs and p were given by Spearman's correlation analysis.

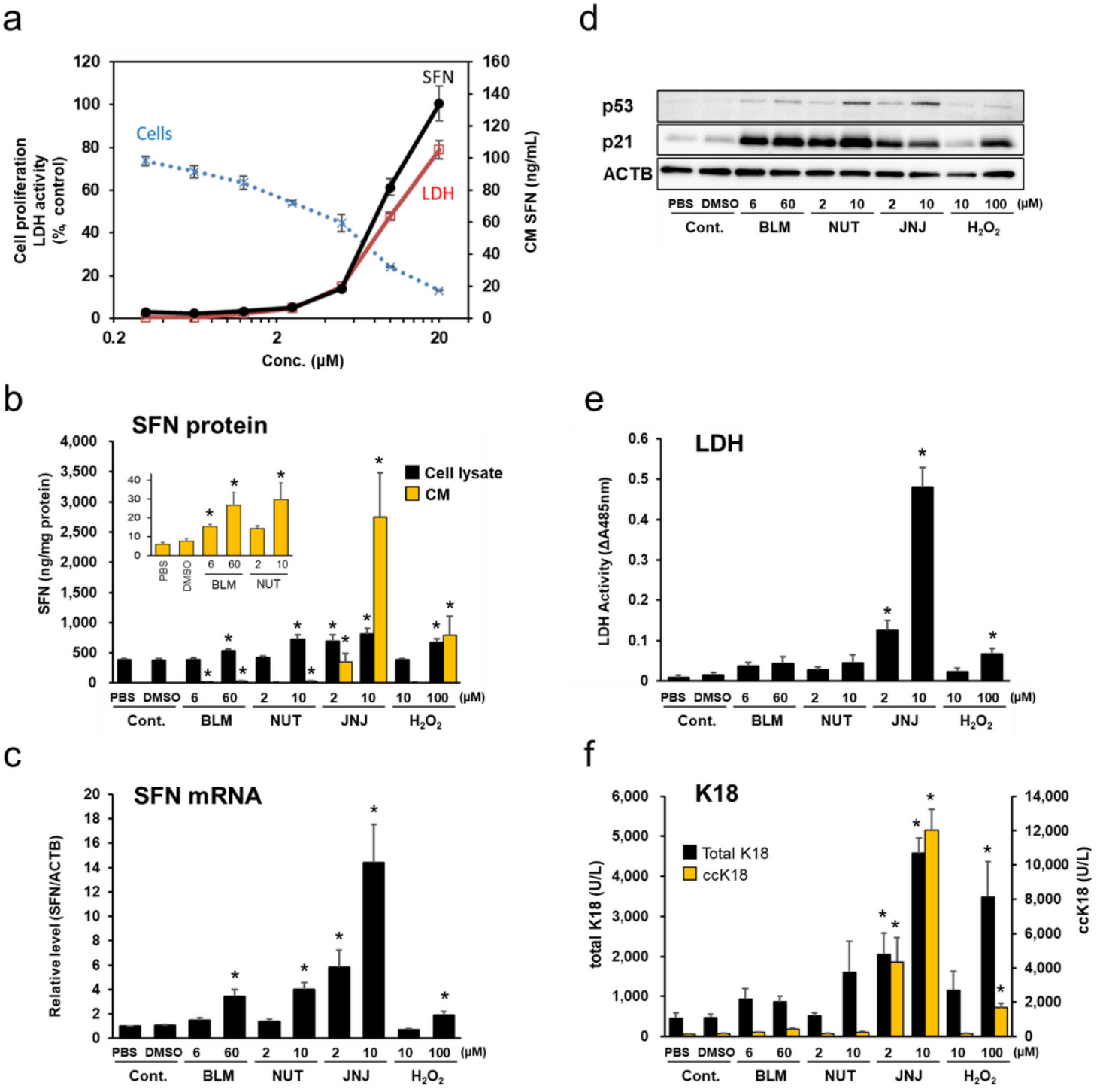

Figure 6

Extracellular release of SFN in vitro. a Dose-dependent SFN expression by JNJ26854165 treatment. Various concentrations of JNJ26854165 were added to the A549 cells. After 48 h, the cell proliferation and the levels of SFN and LDH released into the conditioned medium (CM) were measured. b Comparison of the SFN levels in the conditioned media (CM) and cell lysate. The A549 cells were treated with bleomycin (BLM), nutlin-3 (NUT), JNJ26854165 (JNJ) and H2O2 for 48 h, and then the SFN levels were measured by ELISA. The amounts of SFN relative to the total amounts of proteins in cell lysates are shown. The CM SFN levels stimulated by BLM and NUT are enlarged and inlet at the top left of the graph. c The SFN mRNA levels were measured by qRT-PCR. ACTB (β-actin) was used for normalization. d Comparison of the expression levels of p53 and p21 proteins. Representative results of Western blot are shown. e, f LDH, K18 and ccK18 levels in CM. Three to five independent experiments were performed for each measurement. Standard errors are shown as error bars. A vehicle control was used for each drug (DMSO for BLM, NUT, and JNJ, and PBS for H2O2). Statistically significant differences ($p<0.05$) by t-test in relation to the vehicle control are indicated with an asterisk (*).

Supplementary Files

This is a list of supplementary files associated with this preprint. Click to download.

- supplementarymaterials.pdf